



RESEARCH ARTICLE

WILEY

Transient perturbation of the left temporal cortex evokes plasticity-related reconfiguration of the lexical network

Jana Klaus^{1,2,3} | Dennis J. L. G. Schutter^{1,3} | Vitória Piai^{1,4}

¹Donders Institute for Brain, Cognition and Behavior, Radboud University, Nijmegen, Netherlands

²Max Planck Institute for Human Cognitive and Brain Sciences, Leipzig, Germany

³Helmholtz Institute, Experimental Psychology, Utrecht University, Utrecht, Netherlands

⁴Donders Centre for Medical Neuroscience, Radboud University Medical Center, Nijmegen, Netherlands

Correspondence

Jana Klaus, Max Planck Institute for Human Cognitive and Brain Sciences, Stephanstr. 1A, 04103 Leipzig, Germany.
Email: janaklaus.research@gmail.com

Vitória Piai, Radboud University, Donders Institute for Brain, Cognition and Behavior, Donders Centre for Cognition, P.O. Box 9104, 6500 HE Nijmegen, Netherlands.
Email: v.piai@donders.ru.nl

Funding information

Deutsche Forschungsgemeinschaft, Grant/Award Number: KL 2933/2-1; Nederlandse Organisatie voor Wetenschappelijk Onderzoek, Grant/Award Number: 451-17-003

Abstract

While much progress has been made in how brain organization supports language function, the language network's ability to adapt to immediate disturbances by means of reorganization remains unclear. The aim of this study was to examine acute reorganizational changes in brain activity related to conceptual and lexical retrieval in unimpaired language production following transient disruption of the left middle temporal gyrus (MTG). In a randomized single-blind within-subject experiment, we recorded the electroencephalogram from 16 healthy participants during a context-driven picture-naming task. Prior to the task, the left MTG was perturbed with real continuous theta-burst stimulation (cTBS) or sham stimulation. During the task, participants read lead-in sentences creating a constraining (e.g., "The farmer milks the") or nonconstraining context (e.g., "The farmer buys the"). The last word was shown as a picture that participants had to name (e.g., "cow"). Replicating behavioral studies, participants were overall faster in naming pictures following a constraining relative to a nonconstraining context, but this effect did not differ between real and sham cTBS. In contrast, real cTBS increased overall error rates compared to sham cTBS. In line with previous studies, we observed a decrease in alpha-beta (8–24 Hz) oscillatory power for constraining relative to nonconstraining contexts over left temporal-parietal cortex after participants received sham cTBS. However, following real cTBS, this decrease extended toward left prefrontal regions associated with both domain-general and domain-specific control mechanisms. Our findings provide evidence that immediately after perturbing the left MTG, the lexical-semantic network is able to quickly reconfigure, also recruiting domain-general regions.

KEYWORDS

cortical reorganization, cTBS, EEG, language production

1 | INTRODUCTION

In the past decades, much progress has been made in understanding how the brain is organized to support language functioning (Hickok & Poeppel, 2007; Jackson, Bajada, Rice, Cloutman, & Lambon Ralph,

2018; Poeppel, 2014; Price, 2010; Price, 2012; Tzourio-Mazoyer, Perrone-Bertolotti, Jobard, Mazoyer, & Baciú, 2017). However, the network's ability to adapt to disturbances by means of reorganization remains unclear (Duffau, 2018; Hartwigsen, 2018; Kiran & Thompson, 2019). The investigation of language-network reorganization following

This is an open access article under the terms of the Creative Commons Attribution License, which permits use, distribution and reproduction in any medium, provided the original work is properly cited.

© 2019 The Authors. *Human Brain Mapping* published by Wiley Periodicals, Inc.

left-hemispheric lesions has been largely fueled in the domain of chronic stroke, a time in which autonomous reorganization has already occurred, shadowing immediate adaptation processes (Vaidya, Pujara, Petrides, Murray, & Fellows, 2019). In this domain, one of the ongoing debates concerns the question whether recruitment of homotopic contralateral (i.e., right-hemispheric) areas after left-hemispheric stroke is adaptive or maladaptive for language recovery (Cocquyt, De Ley, Santens, Van Borsel, & De Letter, 2017; Hartwigsen & Saur, 2017; Turkeltaub et al., 2012). Additionally, it has been proposed that domain-general systems may help compensate for focal, domain-specific dysfunction (Geranmayeh, Brownsett, & Wise, 2014; Hartwigsen, 2018). Within this framework, lesions in language-relevant regions trigger an upregulation of intact, domain-general networks, particularly within the so-called Multiple Demand Network (MDN). The MDN is generally assumed to be engaged in tasks requiring general cognitive abilities like inhibition, attentional control, cognitive flexibility, and intelligence, necessitating top-down control (Duncan, 2010; Duncan & Owen, 2000; Fedorenko, Duncan, & Kanwisher, 2012), but is not involved in overlearned tasks. Supporting this framework, activity in prefrontal regions has been related to increased task difficulty, both in healthy and brain-lesioned individuals (Geranmayeh et al., 2014; Piai, Roelofs, Acheson, & Takashima, 2013; Vaden et al., 2013). Assuming that lesions to language-specific brain regions likewise increase the difficulty to perform a linguistic task, domain-general regions could very well compensate for (part of) the required functioning to support behavior, minimizing performance impediments.

One avenue for understanding mechanisms of transient network adaptation is through applying noninvasive brain stimulation inhibitory protocols, like continuous theta-burst stimulation (cTBS), to induce a focal and temporary disruption of a targeted cortical node in the language network, thus implementing neuromodulatory processes. Critically, this is not equivalent to actual damage caused by stroke. First, cTBS causes a spatially distinct downregulation of a circumscribed region, whereas stroke-associated lesions are typically much more diffuse and affect both gray and white matter structures. Second, cTBS, although primarily disruptive in nature, can both impair and improve performance, whereas structural brain lesions typically lead only to performance decrements. Thus, cTBS can serve as a tool to dysregulate healthy network function, opening a window to understanding principles of adaptation on the behavioral and neuronal level in a more controlled manner.

Importantly, the majority of the empirical work regarding cortical reorganization following transient perturbation or real lesions has been conducted using functional magnetic resonance imaging, which provides an indirect (i.e., metabolic) measure of neuronal activity (Logothetis & Wandell, 2004) on a rough temporal scale in the order of seconds (but see Cipollari et al., 2015; Dammekeens, Vanneste, Ost, & De Ridder, 2014; Sarasso et al., 2014 for work combining electrophysiological and neuromodulatory techniques in aphasia, and Tang et al., 2018; Woźniak-Kwaśniewska, Szekely, Aussedat, Bougerol, & David, 2014 for evidence of the effect of cTBS on electrophysiological responses). As such, it remains largely unknown whether the activity observed outside of the left-hemisphere language network is concurrent with task-related, language-network activity or whether it emerges

after the language system has failed. This question can be answered using electrophysiological measures, and in particular oscillations, which provide a window into the dynamic activity of brain regions relevant for language processes at the subsecond time scale and thus enable us to investigate the immediate reorganization processes taking place after a focal perturbation.

In the current study, we combined for the first time a perturbation approach to healthy speakers' brains with electroencephalography (EEG) at the scalp and source levels during a picture-naming task. In this task, participants read lead-in sentences which create a constraining (e.g., "the former milks the") or nonconstraining (e.g., "the farmer buys the") context for a picture (e.g., cow) which subsequently needs to be named. This paradigm has been used in several language-production electrophysiological studies to examine retrieval of concepts and words from memory in a more naturalistic manner that resembles a conversation (Griffin & Bock, 1998), rather than triggered by a picture (Piai, Roelofs, & Maris, 2014; Piai, Roelofs, Rommers, & Maris, 2015; Piai, Rommers, & Knight, 2018). Moreover, this paradigm has previously provided robust and replicable behavioral and electrophysiological effects in both healthy and brain-lesioned participants (Piai et al., 2015; Piai et al., 2018; Piai, Meyer, Dronkers, & Knight, 2017), lending itself ideal to potential modulation induced by noninvasive brain stimulation.

Prior to the task, real or sham cTBS was applied to the left middle temporal gyrus (MTG), a key region for lexical retrieval (Baldo, Arévalo, Patterson, & Dronkers, 2013). Real cTBS causes a controlled, focal reduction in neural excitability of the target region, which is not confounded by long-term reorganization in the chronic phase of a language disorder. In combination with EEG, this allows for a time-sensitive neuronal investigation of immediate adaptive effects in the otherwise undamaged brain. Note that, although cTBS does not prompt changes in neural states equivalent to those produced by stroke, it does cause lasting suppression of neuronal excitability in the targeted region (Siebner & Rothwell, 2003) of about 50 min following application (Wischniewski & Schutter, 2015). Thus, it serves as a proxy to study transient downregulation of a specific area in healthy brain networks.

Behaviorally, we expected a performance decrease in the naming task following real as opposed to sham TMS as a direct marker of the disturbance of the language network. However, we did not expect a modulation of the context effect as a function of the stimulation condition, as this is also not implied by previous studies with lesioned patients using the same paradigm (Piai et al., 2017; Piai et al., 2018). Importantly, the crucial question was how the oscillatory power modulation in the alpha and beta bands (8–25 Hz), as previously observed in the healthy and reorganized brain after left-hemispheric lesions (Piai et al., 2014; Piai et al., 2015; Piai et al., 2017; Piai et al., 2018), would be affected by the focal perturbation. Following lesion evidence, the oscillatory pattern might shift to the right hemisphere (Piai et al., 2017). Using the same task as in the current study, Piai et al. (2017) observed power decreases in the alpha-beta range in the intact right hemisphere in patients with chronic left temporal lesions, suggesting that contralateral regions are recruited when left-hemispheric language nodes are damaged. Alternatively, perilesional networks might get activated in

response to the acute focal perturbation, indicating that acute cortical adaptation is confined to the lesioned hemisphere, where disturbance to function is compensated by other network nodes (Hartwigsen, 2018).

2 | METHODS

2.1 | Participants

Following previous studies (Piai et al., 2014; Piai et al., 2015), we recruited 16 participants. We calculated the smallest population effect size we would be able to detect with this sample size at an alpha-level of .05 and 80% power (with the R *pwr* package, Champely, 2017), which was $d = 0.749$. The present study was deemed sufficiently powered since the behavioral effect in previous studies had an effect size of $d > 2.29$ (Piai et al., 2015; Piai et al., 2017) and the EEG effect has a typical effect size of $d > 0.80$ (Piai et al., 2015).

All participants were right-handed, native Dutch speakers (two male, mean age = 23.0 years, $SD = 3.7$). Exclusion criteria were a family history of epilepsy, an average use of more than three alcoholic beverages daily, use of psychotropic medication or recreational drugs, skin disease, pregnancy, serious head trauma or brain surgery, neurological or psychiatric disorders, large and/or ferromagnetic metal parts in the head (except for a dental wire), implanted cardiac pacemaker or neurostimulator. All participants gave written informed consent prior to the study, which was approved by the local ethics committee of the Radboud University Medical Centre in Nijmegen (NL64141.091.17). Finally, all participants took part in a TMS study for the first time, rendering them maximally naïve to the expected noxious sensation as well as potential behavioral modulations caused by the stimulation protocol.

2.2 | Materials

We employed the context-driven picture naming task used in previous studies (Piai et al., 2014; Piai et al., 2015; Piai et al., 2017; Piai et al., 2018). Two hundred pictures were selected which served as target stimuli. Each picture was associated with two sets of sentences for which the picture names were the last word of the sentences. In the constraining condition, sentences were chosen such that the picture name was highly expected as the final word of the sentence (e.g., “the farmer milks the”), whereas in the non-constraining condition, no one particular word was expected in this position (e.g., “the farmer buys the”). Pictures were allocated to two experimental lists (100 pictures per list corresponding to 200 sentences) to avoid picture repetition across the two experimental sessions. There was no significant difference in sentence length between experimental conditions (constraining: $M = 6.86$, $SD = 1.87$; nonconstraining: $M = 6.73$, $SD = 1.69$; $p > .109$) or experimental lists (List 1: $M = 6.86$, $SD = 1.87$; List 2: $M = 6.73$, $SD = 1.69$; $p > .449$).

2.3 | Design and procedure

The design consisted of the two factors sentence context (constraining vs. nonconstraining) and stimulation condition (real vs. sham). Sentence context and stimulation condition were fully crossed and tested within participants, with the order counterbalanced between sessions.

Stimulus presentation and response recording was controlled by Presentation (Neurobehavioral Systems, Albany, CA). After EEG preparation, individual resting motor threshold (RMT) for the left hemisphere was determined, followed by the application of neuronavigated cTBS. Immediately afterwards, participants were seated in front of a computer screen. After a short practice block, in which participants were trained to read the sentences and name the pictures without collateral blinking, the experimental task was performed in eight blocks each containing 25 trials. At the beginning of an experimental trial, a fixation cross was presented for 500 ms. Then, each word of the sentence was presented for 300 ms, separated by a blank screen of 200 ms. After the last word, a blank screen appeared for 800 ms, followed by the presentation of the target picture for 1,000 ms. Before the next trial was initiated, three asterisks were presented in the center of the screen for 2,000 ms, indicating that participants could blink during this period (Figure 1).

2.3.1 | EEG acquisition

EEG was recorded from 32 Ag/AgCl preamplified scalp electrodes (Biosemi, Amsterdam, The Netherlands) mounted in an elastic cap according to the extended 10–20 system. EEG was sampled at 1,024 Hz. The cap was put on the participants' heads and repositioned using a measuring tape such that the center of the cap and of the head were aligned. The electrooculogram was recorded horizontally from two electrodes placed on the external canthi of both eyes, and vertically from Fp2 and an electrode placed below the right eye.

2.3.2 | Continuous theta-burst stimulation

Neuronavigated cTBS (Localite, Sankt Augustin, Germany) was used to navigate the TMS coil and maintain its exact location and orientation for the duration of the stimulation. A figure-of-eight-shaped coil (double 75 mm; coil type MCF-B65) connected to a MagPro X100 stimulator (MagVenture, Farum, Denmark) was used in all cTBS conditions. The stimulation site was based on MNI coordinates corresponding to the region in which all of the patients in Piai et al. (2017) showed damage (i.e., left MTG; MNI: $x = -63$, $y = -26$, $z = -2$, see Figure 1b). The participants' position and skull shape was registered in space and transformed to a standard brain, allowing for a precise localization of the target region. Session order (real and sham cTBS) was counterbalanced across participants. During real cTBS, we applied 600 biphasic pulses at 50 Hz in trains of three pulses at an interburst interval of 200 ms for 40 s.

For sham cTBS, the same protocol was administered, but the coil was tilted 90° to mimic the auditory sensation of real cTBS while at the same time preventing current from entering the brain.

Stimulation intensity was set at 80% of the individual RMT of the left hemisphere as opposed to the standard 80% of individual active motor threshold (AMT; Huang, Edwards, Rounis, Bhatia, & Rothwell, 2005). We chose this intensity because previous work has shown that the efficacy of cTBS protocols may depend on the intensity used (see for discussion Wischniewski & Schutter, 2015). In particular, the standard cTBS protocol is optimized for decreasing excitability in the motor cortex, whereas the same protocol may result in smaller or shorter effects when applied to other regions of the brain (Goldsworthy, Pitcher, & Ridding, 2012; Gratton, Lee, Nomura, & D'Esposito, 2013; Ishikawa et al., 2007; Rai, Premji, Tommerdahl, & Nelson, 2012). Nyffeler et al. (2006) showed that applying cTBS at 80% RMT over the right frontal eye field successfully modulated performance in an oculomotor task. Brückner, Kiefer, and Kammer (2013) demonstrated that performance on a semantic task is decreased only following cTBS over the left superior temporal cortex at 90% AMT, but not at 80% AMT. Based on this evidence, an intensity higher than the one used with the standard protocol was necessary to exert the excitability-modulating effect over the left temporal gyrus.

Individual RMT was determined using a standardized estimation procedure (Schutter & van Honk, 2006). Participants were seated upright and asked to place the arm contralateral to the stimulation site on the upper leg with the palm of the hand facing upwards. The coil was initially placed over M1. By moving the coil in different directions by approximately 1 cm and gradually increasing TMS intensity, the site for eliciting reliable thumb twitches (five out of five) was localized. Next, intensity was decreased until five out of ten consecutive pulses induced a visually identifiable twitch. Finally, the coil was moved again over the scalp and single TMS pulses were applied to make sure no additional scalp site that surpasses the 50% thumb movement criterion was overlooked. If such a site was found, TMS intensity was further decreased according to the 50% criterion. Mean RMT values were 58.96% ($SD = 8.16$; mean realized coil current gradient = 90 A/us, range: 77–103) of mean stimulator output (MSO), corresponding to an average stimulation intensity of 47.25% ($SD = 6.56$; mean realized coil current gradient = 72 A/us, range: 61–83).

2.3.3 | Behavioral analysis

All analyses were performed using R (version 3.4.1; www.r-project.org). Responses were coded offline for accuracy, and trials in which a wrong or no utterance was produced, or where an utterance was corrected, were removed from the RT analysis (corresponding to 3.8% of the total data). For correct responses, naming latencies were measured manually using Praat (Boersma & Weenink, 2018). Naming latencies were analyzed using linear mixed effects models in the lme4 package (version 1.1.13; Bates, Mächler, Bolker, & Walker, 2015). Error rates were analyzed using generalized linear mixed

effects models (GLMEM). For all analyses, we included by-participant intercepts to account for interindividual variability in overall task performance, as well as by-participant slopes for the main effect of cTBS. Additionally, we included a by-participant and by-item slope for sentence context. The α -level was set to .05 (two-tailed) for all analyses.

2.3.4 | EEG analysis

All analyses were performed using FieldTrip version 20171203 (Oostenveld, Fries, Maris, & Schoffelen, 2011) in MatlabR2017a. Trials removed from the RT analysis were also removed from the EEG analysis. Each electrode was re-referenced offline to averaged mastoids. The data were high-pass filtered at 0.16 Hz and segmented into time epochs corresponding to a time window ranging from 1,000 ms pre-picture onset to 300 ms post-picture onset. All epochs were inspected individually for eye movements, blinks, and other artifacts blinded for condition (see for discussion Cohen, 2017), and trials containing artifacts were removed from the analysis (236 trials in total, 3.7% of the data). Furthermore, excessively noisy channels in individual participants were repaired by spherical spline interpolating (Perrin, Pernier, Bertrand, & Echallier, 1989). Subsequently, for the time-frequency representations time-resolved power was calculated with a modified spectrogram approach (Bruns, 2004) for frequencies ranging from 2 to 30 Hz at the single-trial level (FieldTrip method "mtmconvol"). For that, an adaptive time window of frequency-specific three cycles' length was slid over the signal, advanced in steps of 10 ms in the temporal dimension and in steps of 1 Hz in the frequency dimension. The data in each window was multiplied with a Hanning taper, followed by the Fourier transform from the resulting tapered signal. Time-frequency representations were then averaged per participant and context by stimulation condition.

2.3.5 | Source-level analysis

For the source-level analysis, the scalp data were re-referenced offline using the common average reference. Source-level power was estimated for each participant based on the scalp-level cluster properties (see Section 3), that is, –700 ms to –100 ms relative to picture onset and 16 Hz center frequency, using the dynamic imaging of coherent sources method (Gross et al., 2001). A standard boundary element method volume conduction model was used (Oostenveld, Stegeman, Praamstra, & van Oosterom, 2003). The position of the electrodes was checked for alignment with the volume conduction model based on the center of the head and the preauricular points. The volume was discretized into a grid (1 cm resolution) and the leadfield matrix was calculated for each grid point. The cross-spectral density matrix was computed between 8 and 24 Hz (i.e., spectral smoothing of 8 Hz). The cross-spectral density and leadfield matrices were used to compute common spatial filters (i.e., over both conditions) at each location of the 3D-grid. The common spatial filters were subsequently applied

to the Fourier transformed data from each condition separately to obtain source-level spectral power estimates for each grid point. Source-level spectral power estimates were averaged per participant and context by stimulation condition.

2.3.6 | EEG statistical analyses

The differences in spectral power between conditions for each stimulation type were evaluated using a nonparametric cluster based permutation procedure, which effectively controls the false alarm rate, at both the scalp and source levels (Maris & Oostenveld, 2007). At the scalp level, the tests were performed on all available channels, time points, and frequencies (i.e., 2–30 Hz). We did not define specific frequency bands a priori because the distinction between the alpha and beta bands is not always clear cut in certain cognitive domains (Donner & Siegel, 2011; for discussion in the domains of memory and language see Piai & Zheng, 2019). At the source level, the tests were performed over all grid points. Clusters were identified of adjacent data points that exhibited a similar difference between the two conditions across participants based on a two-tailed dependent-samples

t tests at an α -level of .05. Cluster-level statistics were calculated from the summed t values within each cluster. Statistical significance was obtained with Monte Carlo stimulations (10,000 random partitions). We assessed the context effect (constraining vs. nonconstraining) averaged over both cTBS conditions, and also for each cTBS condition separately. At the scalp level, the interaction between context and cTBS condition was assessed by calculating the relative difference between context conditions for each cTBS condition separately, and then comparing those relative differences directly.

3 | RESULTS

3.1 | Left MTG perturbation increases errors in context-driven word retrieval

Figure 2 displays mean naming latencies and error rates broken down by context condition (constraining vs. nonconstraining) and cTBS condition (real vs. sham). Following sham cTBS, participants' mean RTs were 525 ms ($SD = 215$) in the constraining and 704 ms ($SD = 180$) in the nonconstraining condition. Following real cTBS, participants' mean

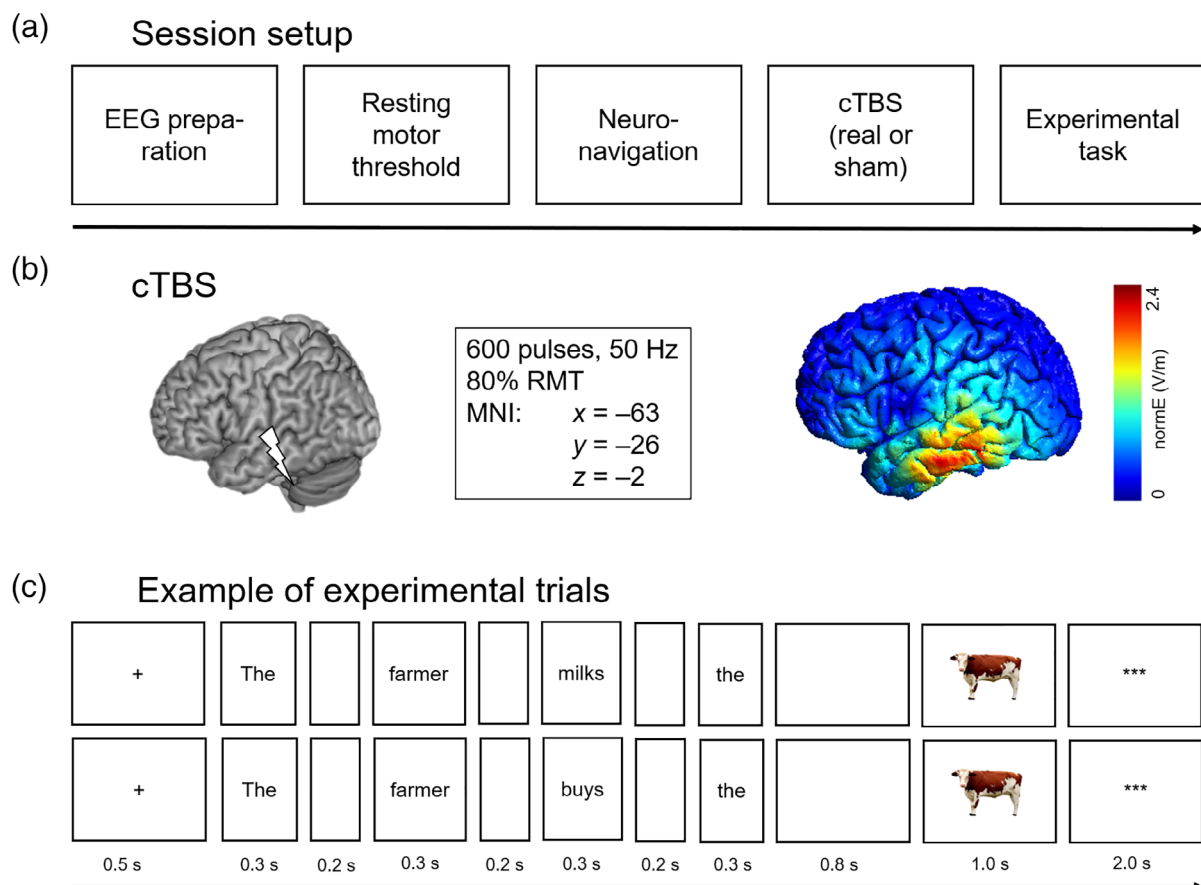


FIGURE 1 Overview of the experimental procedures. (a) Schematic illustration of an experimental session. (b) Illustration of the cTBS target site (left) and the induced magnetic field as simulated in an example brain using SimNIBS (version 2.0; Thielscher et al., 2015) (right). (c) Two example trials illustrating the constraining context condition (top) and nonconstraining context condition (bottom), respectively

RTs were 521 ms ($SD = 204$) in the constraining and 695 ms ($SD = 178$) in the nonconstraining condition. Responses in the constraining condition were reliably faster than in the nonconstraining condition ($\beta = 90.44$, $SE = 7.20$, $t = 12.56$, $p < .0001$, $d = 0.92$), replicating the context effect from previous studies. There was no difference in overall naming latencies as a function of cTBS condition ($\beta = -4.35$, $SE = 4.73$, $t = -0.92$, $p = .372$, $d = 0.04$). Furthermore, the size of the context effect was comparable following real and sham cTBS ($\beta = 0.19$, $SE = 2.32$, $t = 0.08$, $p = .950$, $d < 0.01$).

Following sham cTBS, participants' error rates were 1.8% ($SD = 1.4$) and 2.3% ($SD = 1.5$) for the constraining and nonconstraining condition, respectively. Following real cTBS, participants made 2.7% ($SD = 1.7$) errors in the constraining and 3.4% ($SD = 1.8$) errors in the nonconstraining condition. In the GLMEM analysis, the maximal model as specified in the Methods section did not converge. Thus, we

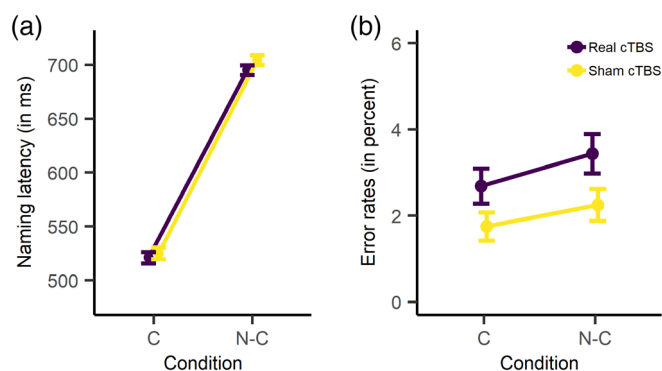


FIGURE 2 Behavioral results. (a) Mean naming latencies (in ms), broken down by cTBS condition (real vs. sham) and context condition (constraining vs. nonconstraining). (b) Error rates (in percent), broken down by cTBS condition (real vs. sham) and context condition (constraining vs. nonconstraining). C = constraining; N-C = nonconstraining. Error bars represent standard errors of the mean

reduced the random-effects structure, which resulted in a final model that contained by-participant and by-item intercepts. In this model, error rates did not differ between the constraining and the nonconstraining condition ($\beta = 0.13$, $SE = 0.08$, $z = 1.60$, $p = .110$, odds ratio = 1.14, 95% CI: 0.97–1.35). Participants made more errors following real compared to sham cTBS ($\beta = 0.23$, $SE = 0.08$, $z = 2.73$, $p = .006$, odds ratio = 1.26, 95% CI: 1.07–1.49). Context condition and stimulation condition did not interact ($\beta = 0.00$, $SE = 0.08$, $z = 0.01$, $p = .995$, odds ratio = 1.00, 95% CI: 0.85–1.18).

3.2 | Left MTG perturbation modulates prepicture alpha-beta oscillations

Across both real and sham cTBS conditions, power decreases were stronger following constraining relative to nonconstraining contexts (Monte Carlo $p = .001$). Moreover, we also assessed the context effect for each cTBS condition separately, as shown in Figure 3. Following sham cTBS, a statistically significant cluster was found (Monte Carlo $p = .003$). Here, power decreases were most prominent between 8 and 24 Hz and between 700 and 100 ms prior to picture onset over all 32 channels tested, with the strongest decreases over left posterior and left and right anterior channels (see left panel of Figure 3), replicating previous findings. We note that this effect comprises both the classical alpha and beta frequency bands, a point to which we will return in the discussion. These results remained virtually identical when the alpha (8–15 Hz) and beta (16–30 Hz) bands were tested separately with cluster-based permutation (for alpha, Monte Carlo $p = .008$; for beta, Monte Carlo $p = .005$). By contrast, following real cTBS, this context effect was attenuated, resulting in no significant clusters over the scalp (Monte Carlo $p = .087$). Looking at the group-level time-frequency representations broken down by cTBS condition (Figure 3) revealed differences in the topographical distribution of the context effect, implying a different neuronal configuration of the

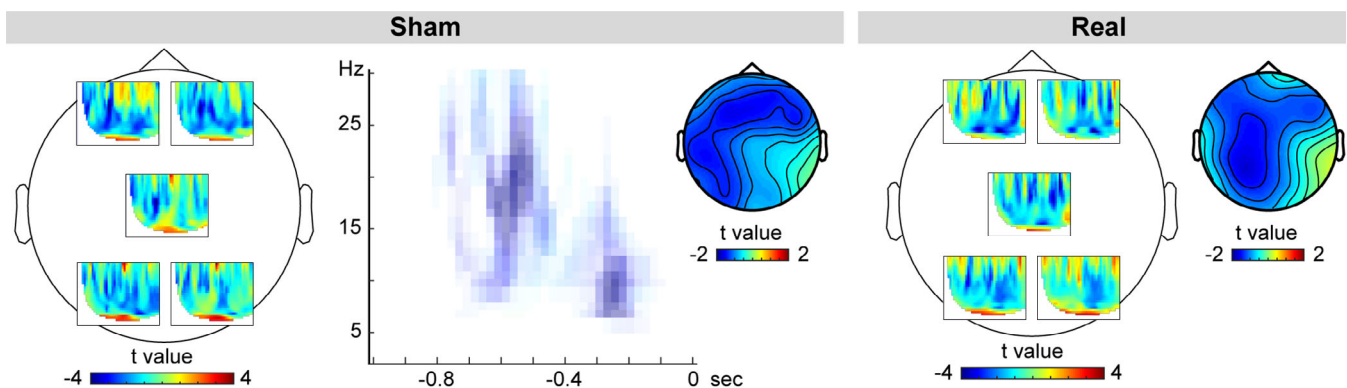
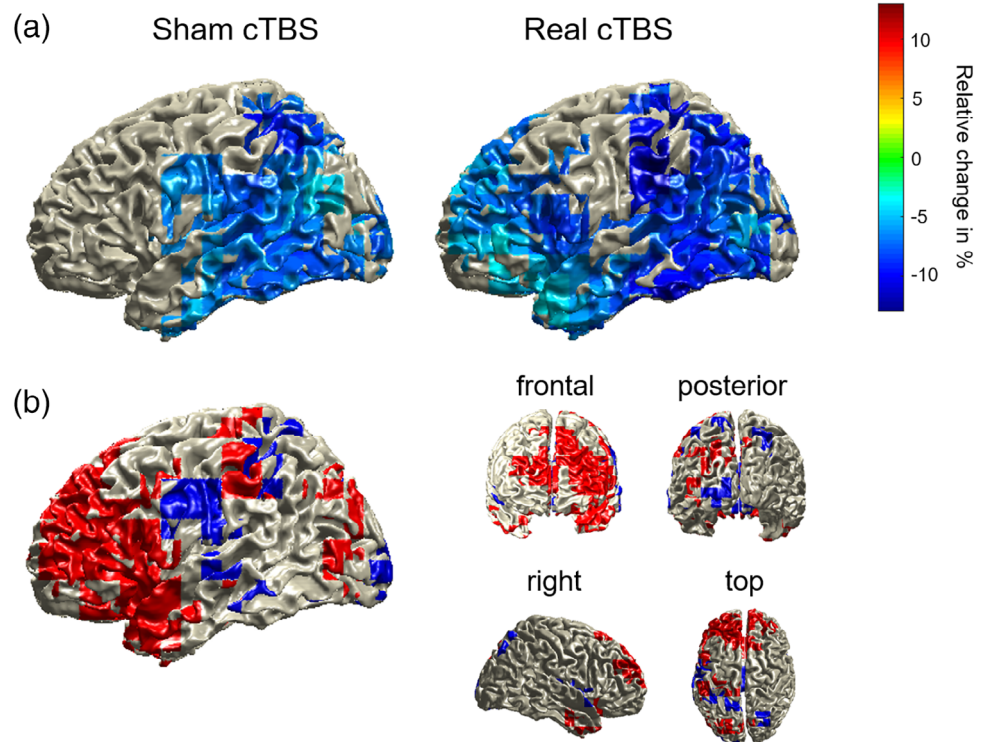


FIGURE 3 Group-level time-frequency representation and scalp distribution of the power changes for the constraining relative to the nonconstraining condition, broken down by cTBS condition. T-values for the comparison between time-resolved spectra are shown for five representative channels. The location of each time-resolved spectra corresponds roughly to the location of the respective channel. For sham cTBS, the significant cluster is shown averaged over the channels belonging to the cluster (i.e., all 32 channels assessed); data points not pertaining to the cluster are masked. Scalp topographies are shown for the averages between 8 and 24 Hz and -700 and -100 ms

FIGURE 4 (a) Source localization of the power decreases for constraining relative to nonconstraining contexts (displayed in relative percent change) for both cTBS conditions, masked by the statistically significant grid points. (b) Difference plot displaying suprathreshold source-level activity specific for real cTBS (red) and sham cTBS (blue)



underlying sources for sham versus real cTBS. The interaction between cTBS and context condition was not significant (Monte Carlo $p = .980$). However, we note that cluster-based permutation testing is appropriate for assessing the hypothesis of exchangeability across the conditions tested, but not for inferring specific spatial-spectrotemporal differences between conditions (Maris & Oostenveld, 2007). Therefore, to follow up on the spatial differences between cTBS conditions, we localized the neuronal sources of the context effect for each condition separately.

3.3 | Left MTG perturbation causes additional recruitment of left prefrontal regions

The difference in scalp topographies between the cTBS conditions implies distinct patterns of neuronal generators. To allow for an anatomically more defined comparison between the two cTBS conditions, we source-localized participants' context effects using frequency-domain beamformers across the time-frequency window found to elicit the strongest power decrease at the scalp level for sham stimulation and for both cTBS conditions combined (i.e., 700–100 ms prior to picture onset and from 8 to 24 Hz). Power decreases in this time-frequency range were statistically significant following sham cTBS ($p = .008$) as well as real cTBS ($p = .002$). The source results, displayed as relative power decreases separated by cTBS condition, are shown in Figure 4a. Following sham cTBS, the context effect was localized in left temporal and parietal regions, replicating previous findings from MEG (Piai et al., 2015). By contrast, following real cTBS, this effect was much more widespread toward left prefrontal regions,

additionally encompassing the left frontal cortex and anterior temporal lobe. Figure 4b displays the source differences between the two cTBS conditions, illustrating which regions were selectively recruited following sham (blue) and real (red) cTBS. Left prefrontal regions were selectively recruited following real cTBS. By contrast, following sham cTBS, only comparably small portions of the left precentral gyrus were selectively recruited.

4 | GENERAL DISCUSSION

The goal of the present study was to investigate the immediate effects of a downregulation of the midsection of the left temporal gyrus on the behavioral performance as well as on the time-resolved oscillatory patterns of context-guided language production. Transiently perturbing activity in the left MTG with high-frequency cTBS prior to the task effectively disrupted the contribution of this node within the semantic language production network. Behaviorally, this translated into an increase in overall task difficulty, as shown by an increase in picture naming error rates, regardless of whether the to-be-named picture was expected or not. Picture naming latencies showed the facilitation effect from sentence context irrespective of cTBS condition. Thus, real cTBS affected language *production*, rather than comprehension.

At the neuronal level, the sham condition replicated previous findings of power decreases in the alpha-beta band in left temporal and inferior parietal regions prior to picture onset (Piai et al., 2014; Piai et al., 2015; Piai et al., 2017; Piai et al., 2018). In line with previous literature, this effect did not respect the classical boundary

between the alpha and beta bands when tested over the entire frequency range (see for discussion Piai & Zheng, 2019). By contrast, the left MTG perturbation resulted in attenuated scalp effects and, at the source level, additional recruitment of left prefrontal regions concurrent with the left posterior activity.

Previous studies have shown that a rise in task difficulty is associated with stronger activity in left ventro- and dorsolateral prefrontal cortex and the cingulo-opercular network, which encompasses the dorsal anterior cingulate cortex, superior frontal gyrus, and sometimes posterior inferior frontal gyrus (Brownsett et al., 2014; Camilleri et al., 2018; Erb, Henry, Eisner, & Obleser, 2013; Fedorenko, Behr, & Kanwisher, 2011; Fedorenko, Duncan, & Kanwisher, 2013; Fridriksson & Morrow, 2005; Geranmayeh et al., 2014; Piai et al., 2013; Vaden et al., 2013). Our source-level analysis of task-specific oscillatory activity is in line with these previous findings, suggesting recruitment of the domain-general control network (e.g., left middle and superior frontal gyrus), next to regions that have been associated with domain-general and domain-specific processing like the left inferior frontal gyrus, in the face of higher task demands. Importantly, using electrophysiological measures and, in particular, analyses of oscillatory activity, we were able to demonstrate that these left prefrontal areas are engaged in the same time scale (i.e., in less than a second) as the left posterior areas, rather than (s) later in time. The left prefrontal regions also become integrated into the same oscillatory band. This finding is particularly novel and has substantial implications for understanding mechanisms of network reconfiguration, in that it provides temporally and spatially specific evidence of the concurrent recruitment of “perilesional” regions following a focal perturbation. It is possible that the vicinity of the stimulated region to the inferior fronto-occipital and inferior longitudinal fasciculi connecting left posterior to anterior regions (Duffau et al., 2005; Turken & Dronkers, 2011) facilitated the spread of activity to frontal regions in the real cTBS condition. In other words, these connections may have mediated the integration of the frontal regions as observed in the oscillatory activity, increasing the size of the network in the same frequency band.

Interestingly, we found no evidence that the right hemisphere performs a compensating role when part of the left-hemispheric network is transiently and focally disturbed, as has been reported for healthy participants (Andoh & Paus, 2011; Hartwigsen et al., 2013) as well as chronic aphasic patients with lesions in the left hemisphere (Musso et al., 1999; Piai et al., 2017; Saur et al., 2006; Turkeltaub et al., 2012; Winhuisen et al., 2005). This suggests that in the current study acute responses to focal left-hemispheric perturbation were offset entirely by perilesional regions in the same hemisphere as opposed to homotopic regions (Hartwigsen et al., 2017).

A similar pattern of additional prefrontal cortex recruitment with the same paradigm was observed in an MEG study by Piai et al. (2015), in which healthy volunteers alternated between naming the picture presented at the end of a sentence (i.e., language production, identical to the current task) and judging, via button press, whether the picture was expected or not. This additional task demand (i.e., switching between two different output modes) was reflected in

a similar pattern of additional source activity in the prefrontal cortex during the language production task as obtained in the current study. By contrast, Roos and Piai (in preparation) localized alpha-beta oscillatory activity exclusively to the left temporal lobe with high test-retest reliability when participants only executed the naming task, that is, in the absence of additional higher-order control, and comparable to the sham condition in the current study. Combined, these findings provide further evidence that increased left prefrontal activity may be associated with increased executive control involvement.

It should be noted that typically, the MDN associated with domain-general control is found in both hemispheres, whereas in the current study, the signal was localized predominantly to the left hemisphere. However, based on functional connectivity analyses it was recently proposed that the MDN can be subdivided into different subregions, in which the left inferior frontal junction and left presupplementary motor area as being recruited as domain-general regions in situations where language and speech execution-related processes need to be augmented (Camilleri et al., 2018). Thus, in line with the theoretical framework of the current study, the recruitment of these left-hemispheric regions is expected.

Arguably, the quality of the source localization in the present study is not optimal, as we did not have exact electrode locations nor individual scans for the reconstruction of the sources (Akalin Acar & Makeig, 2013). Despite this caveat, we are confident in the accuracy of our results given the similarity of the observed pattern in left posterior cortex in the sham condition with previous studies (Piai et al., 2015; Roos and Piai, in preparation). Moreover, localization errors resulting from these shortcomings should be in the margin of 10–15 mm (Akalin Acar & Makeig, 2013), whereas the anterior spread we observed extends beyond that. Regardless, caution should be exerted when interpreting the source locations strictly. Ideally, the results should be replicated in future studies with more carefully computed forward models. Nonetheless, the current results support the inference that an increase in task demands, as caused by perturbing an important node in the lexical-semantic network, triggers an immediate recruitment of additional left prefrontal regions, possibly associated with the Multiple Demand Network.

Two limitations of the study need to be discussed. First, we only compared active cTBS over the left MTG to a sham condition as opposed to an active control site. As such, we do not make definitive claims about the anatomical specificity of the error increase observed in the current study. Future studies could investigate whether the effect replicates when an active control region is tested, which would provide stronger evidence that down-regulation of the left MTG causes a performance decrement in lexical retrieval. Second, no control task was tested so we cannot make any claims whether perturbation of the left MTG causes exclusively performance decreases related to language production or whether other, nonverbal functions would be similarly affected. Again, this is an exciting prospect for future research.

The discrepancy between the scalp- and source-level results for the real cTBS condition deserves some attention. Using Monte Carlo

simulations, no reliable oscillatory effect was found at the scalp level following real cTBS, indicating that the effect became more variable across participants in the spatial-spectro-temporal domain. At the source level, however, the effect was reliable across participants (see also Piai et al., 2015 for a similar apparent discrepancy between scalp- and source-level results). This discrepancy can be explained by the fact that beamforming, the source localization method we employed, is a spatial filtering technique which suppresses the contributions of noise sources that are temporally correlated to reconstruct the neuronal sources of an effect of interest (Gross et al., 2001). The scalp-level activity is a conglomerate of many sources of signal/noise. An improved signal-to-noise ratio is expected once spatial filtering is employed, leading to significant effects at the source level as in the current study.

The current results cannot exclude the possibility that the stimulation disrupted lexical retrieval processes exclusively, but instead also affected verbal self-monitoring, which has been localized to the left superior temporal gyrus (Indefrey, 2011; Skipper, Devlin, & Lametti, 2017). This region is anatomically close to and interconnected with our target site, allowing for the possibility of peripheral stimulation effects. In fact, our finding that active cTBS increased overall error rates may also be reconciled with such an assumption. Nevertheless, we assume that the strongest effect of the stimulation was exerted immediately under the coil, very likely disrupting lexical retrieval processes. Future studies could investigate whether tasks designed to tackle verbal self-monitoring are affected in a similar way with the current stimulation setup.

In summary, the current study showed for the first time how behavioral and underlying electrophysiological correlates of language production are affected by transient perturbation of a key region within the semantic network. The findings show that this results in an initiation of adaptive processes of functional networks to left frontal and temporal regions associated with both domain-general as well as domain-specific, lexical-semantic processes. However, this adaptation mechanism was not successful in entirely alleviating performance decrements, as overall error rates were moderately, but significantly increased following real cTBS. Together, these results provide new insights into the cortical mechanisms at play in response to disruption of normal functioning.

ACKNOWLEDGMENTS

This work was supported by the German Research Foundation (grant number KL 2933/2-1 to J. K.) and the Netherlands Organization for Scientific Research (grant number 451-17-003 to V. P.). We would like to thank Anna Dewenter for invaluable assistance in data collection and Gesa Hartwigsen for helpful comments on previous versions of this manuscript.

DATA AVAILABILITY STATEMENT

The data that support the findings of this study are available at the Open Science Framework (<https://osf.io/k7juy/>).

ORCID

Jana Klaus  <https://orcid.org/0000-0003-4398-8672>

REFERENCES

- Akalin Acar, Z., & Makeig, S. (2013). Effects of forward model errors on EEG source localization. *Brain Topography*, *26*, 378–396.
- Andoh, J., & Paus, T. (2011). Combining functional neuroimaging with offline brain stimulation: Modulation of task-related activity in language areas. *Journal of Cognitive Neuroscience*, *23*, 349–361.
- Baldo, J. V., Arévalo, A., Patterson, J. P., & Dronkers, N. F. (2013). Grey and white matter correlates of picture naming: Evidence from a voxel-based lesion analysis of the Boston Naming Test. *Cortex*, *49*, 658–667.
- Bates, D., Mächler, M., Bolker, B., & Walker, S. (2015). Fitting linear mixed-effects models using lme4. *Journal of Statistical Software*, *67*, 1–48.
- Boersma, P., & Weenink, D. (2018). *Praat: Doing phonetics by computer*. <http://www.praat.org/>.
- Brownsett, S. L. E., Warren, J. E., Geranmayeh, F., Woodhead, Z., Leech, R., & Wise, R. J. S. (2014). Cognitive control and its impact on recovery from aphasic stroke. *Brain*, *137*, 242–254.
- Brückner, S., Kiefer, M., & Kammer, T. (2013). Comparing the after-effects of continuous theta burst stimulation and conventional 1 Hz rTMS on semantic processing. *Neuroscience*, *233*, 64–71.
- Bruns, A. (2004). Fourier-, Hilbert- and wavelet-based signal analysis: Are they really different approaches? *Journal of Neuroscience Methods*, *137*, 321–332.
- Camilleri, J. A., Müller, V. I., Fox, P., Laird, A. R., Hoffstaedter, F., Kalenscher, T., & Eickhoff, S. B. (2018). Definition and characterization of an extended multiple-demand network. *NeuroImage*, *165*, 138–147.
- Champely, S. (2017). *pwr: Basic functions for power analysis. R package version 1.2-1*. <https://CRAN.R-project.org/package=pwr>.
- Cipollari, S., Veniero, D., Razzano, C., Caltagirone, C., Koch, G., & Marangolo, P. (2015). Combining TMS-EEG with transcranial direct current stimulation language treatment in aphasia. *Expert Review of Neurotherapeutics*, *15*, 833–845.
- Cocquyt, E.-M., De Ley, L., Santens, P., Van Borsel, J., & De Letter, M. (2017). The role of the right hemisphere in the recovery of stroke-related aphasia: A systematic review. *Journal of Neurolinguistics*, *44*, 68–90.
- Cohen, M. X. (2017). Rigor and replication in time-frequency analyses of cognitive electrophysiology data. *International Journal of Psychophysiology*, *111*, 80–87.
- Dammekens, E., Vanneste, S., Ost, J., & De Ridder, D. (2014). Neural correlates of high frequency repetitive transcranial magnetic stimulation improvement in post-stroke non-fluent aphasia: A case study. *Neurocase*, *20*, 1–9.
- Donner, T. H., & Siegel, M. (2011). A framework for local cortical oscillation patterns. *Trends in Cognitive Sciences*, *15*, 191–199.
- Duffau, H. (2018). The error of Broca: From the traditional localizationist concept to a connectome anatomy of human brain. *Journal of Chemical Neuroanatomy*, *89*, 73–81.
- Duffau, H., Gatignol, P., Mandonnet, E., Peruzzi, P., Tzourio-Mazoyer, N., & Capelle, L. (2005). New insights into the anatomo-functional connectivity of the semantic system: A study using cortico-subcortical electrostimulation. *Brain*, *128*, 797–810.
- Duncan, J. (2010). The multiple-demand (MD) system of the primate brain: Mental programs for intelligent behaviour. *Trends in Cognitive Sciences*, *14*, 172–179.
- Duncan, J., & Owen, A. (2000). Common regions of the human frontal lobe recruited by diverse cognitive demands. *Trends in Neurosciences*, *23*, 475–483.
- Erb, J., Henry, M. J., Eisner, F., & Obleser, J. (2013). The brain dynamics of rapid perceptual adaptation to adverse listening conditions. *The Journal of Neuroscience*, *33*, 10688–10697.

- Fedorenko, E., Behr, M. K., & Kanwisher, N. (2011). Functional specificity for high-level linguistic processing in the human brain. *Proceedings of the National Academy of Sciences*, 108, 16428–16433.
- Fedorenko, E., Duncan, J., & Kanwisher, N. (2012). Language-selective and domain-general regions lie side by side within Broca's area. *Current Biology*, 22, 2059–2062.
- Fedorenko, E., Duncan, J., & Kanwisher, N. (2013). Broad domain generality in focal regions of frontal and parietal cortex. *Proceedings of the National Academy of Sciences*, 110, 16616–16621.
- Fridriksson, J., & Morrow, L. (2005). Cortical activation and language task difficulty in aphasia. *Aphasiology*, 19, 239–250.
- Geranmayeh, F., Brownsett, S. L. E., & Wise, R. J. S. (2014). Task-induced brain activity in aphasic stroke patients: What is driving recovery? *Brain*, 137, 2632–2648.
- Goldsworthy, M. R., Pitcher, J. B., & Ridling, M. C. (2012). A comparison of two different continuous theta burst stimulation paradigms applied to the human primary motor cortex. *Clinical Neurophysiology*, 123, 2256–2263.
- Gratton, C., Lee, T. G., Nomura, E. M., & D'Esposito, M. (2013). The effect of theta-burst TMS on cognitive control networks measured with resting state fMRI. *Frontiers in Systems Neuroscience*, 7, 124.
- Griffin, Z. M., & Bock, K. (1998). Constraint, word frequency, and the relationship between lexical processing levels in spoken word production. *Journal of Memory and Language*, 38, 313–338.
- Gross, J., Kujala, J., Hämäläinen, M., Timmermann, L., Schnitzler, A., & Salmelin, R. (2001). Dynamic imaging of coherent sources: Studying neural interactions in the human brain. *Proceedings of the National Academy of Sciences of the United States of America*, 98, 694–699.
- Hartwigsen, G. (2018). Flexible redistribution in cognitive networks. *Trends in Cognitive Sciences*, 22, 687–698.
- Hartwigsen, G., Bzdok, D., Klein, M., Wawrzyniak, M., Stockert, A., Wrede, K., ... Saur, D. (2017). Rapid short-term reorganization in the language network. *eLife*, 6, e25964.
- Hartwigsen, G., & Saur, D. (2017). Neuroimaging of stroke recovery from aphasia—Insights into plasticity of the human language network. *NeuroImage*, 190, 14–31.
- Hartwigsen, G., Saur, D., Price, C. J., Ulmer, S., Baumgaertner, A., & Siebner, H. R. (2013). Perturbation of the left inferior frontal gyrus triggers adaptive plasticity in the right homologous area during speech production. *Proceedings of the National Academy of Sciences of the United States of America*, 110, 16402–16407.
- Hickok, G., & Poeppel, D. (2007). The cortical organization of speech processing. *Nature Reviews. Neuroscience*, 8, 393–402.
- Huang, Y.-Z., Edwards, M. J., Rounis, E., Bhatia, K. P., & Rothwell, J. C. (2005). Theta burst stimulation of the human motor cortex. *Neuron*, 45, 201–206.
- Indefrey, P. (2011). The spatial and temporal signatures of word production components: A critical update. *Frontiers in Psychology*, 2, 255.
- Ishikawa, S., Matsunaga, K., Nakanishi, R., Kawahira, K., Murayama, N., Tsuji, S., ... Rothwell, J. C. (2007). Effect of theta burst stimulation over the human sensorimotor cortex on motor and somatosensory evoked potentials. *Clinical Neurophysiology*, 118, 1033–1043.
- Jackson, R. L., Bajada, C. J., Rice, G. E., Cloutman, L. L., & Lambon Ralph, M. A. (2018). An emergent functional parcellation of the temporal cortex. *NeuroImage*, 170, 385–399.
- Kiran, S., & Thompson, C. K. (2019). Neuroplasticity of language networks in aphasia: Advances, updates, and future challenges. *Frontiers in Neurology*, 10, 295.
- Logothetis, N. K., & Wandell, B. A. (2004). Interpreting the BOLD signal. *Annual Review of Physiology*, 66, 735–769.
- Maris, E., & Oostenveld, R. (2007). Nonparametric statistical testing of EEG- and MEG-data. *Journal of Neuroscience Methods*, 164, 177–190.
- Musso, M., Weiller, C., Kiebel, S., Müller, S. P., Bülow, P., & Rijntjes, M. (1999). Training-induced brain plasticity in aphasia. *Brain*, 122, 1781–1790.
- Nyffeler, T., Wurtz, P., Lüscher, H.-R., Hess, C. W., Senn, W., Pflugshaupt, T., ... Müri, R. M. (2006). Repetitive TMS over the human oculomotor cortex: Comparison of 1-Hz and theta burst stimulation. *Neuroscience Letters*, 409, 57–60.
- Oostenveld, R., Fries, P., Maris, E., & Schoffelen, J.-M. (2011). FieldTrip: Open source software for advanced analysis of MEG, EEG, and invasive electrophysiological data. *Computational Intelligence and Neuroscience*, 2011, 156869.
- Oostenveld, R., Stegeman, D. F., Praamstra, P., & van Oosterom, A. (2003). Brain symmetry and topographic analysis of lateralized event-related potentials. *Clinical Neurophysiology*, 114, 1194–1202.
- Perrin, F., Pernier, J., Bertrand, O., & Echallier, J. F. (1989). Spherical splines for scalp potential and current density mapping. *Electroencephalography and Clinical Neurophysiology*, 72, 184–187.
- Piai, V., Meyer, L., Dronkers, N. F., & Knight, R. T. (2017). Neuroplasticity of language in left-hemisphere stroke: Evidence linking subsecond electrophysiology and structural connections. *Human Brain Mapping*, 38, 3151–3162.
- Piai, V., Roelofs, A., Acheson, D. J., & Takashima, A. (2013). Attention for speaking: Domain-general control from the anterior cingulate cortex in spoken word production. *Frontiers in Human Neuroscience*, 7, 832.
- Piai, V., Roelofs, A., & Maris, E. (2014). Oscillatory brain responses in spoken word production reflect lexical frequency and sentential constraint. *Neuropsychologia*, 53, 146–156.
- Piai, V., Roelofs, A., Rommers, J., & Maris, E. (2015). Beta oscillations reflect memory and motor aspects of spoken word production. *Human Brain Mapping*, 36, 2767–2780.
- Piai, V., Rommers, J., & Knight, R. T. (2018). Lesion evidence for a critical role of left posterior but not frontal areas in alpha-beta power decreases during context-driven word production. *The European Journal of Neuroscience*, 48, 2622–2629.
- Piai, V., & Zheng, X. (2019). Speaking waves: Neuronal oscillations in language production. *Psychology of Learning and Motivation*, 71, 265–302.
- Poeppel, D. (2014). The neuroanatomic and neurophysiological infrastructure for speech and language. *Current Opinion in Neurobiology*, 28, 142–149.
- Price, C. J. (2010). The anatomy of language: A review of 100 fMRI studies published in 2009. *Annals of the New York Academy of Sciences*, 1191, 62–88.
- Price, C. J. (2012). A review and synthesis of the first 20 years of PET and fMRI studies of heard speech, spoken language and reading. *NeuroImage*, 62, 816–847.
- Rai, N., Premji, A., Tommerdahl, M., & Nelson, A. J. (2012). Continuous theta-burst rTMS over primary somatosensory cortex modulates tactile perception on the hand. *Clinical Neurophysiology*, 123, 1226–1233.
- Roos, N., Piai, V. *Across-session consistency of context-driven language production: a magnetoencephalography study*. In preparation.
- Sarasso, S., Määttä, S., Ferrarelli, F., Poryazova, R., Tononi, G., & Small, S. (2014). Plastic changes following imitation-based speech and language therapy for aphasia: A high-density sleep EEG study. *Neurorehabilitation and Neural Repair*, 28, 129–138.
- Saur, D., Lange, R., Baumgaertner, A., Schraknepper, V., Willmes, K., Rijntjes, M., & Weiller, C. (2006). Dynamics of language reorganization after stroke. *Brain*, 129, 1371–1384.
- Schutter, D. J. L. G., & van Honk, J. (2006). A standardized motor threshold estimation procedure for transcranial magnetic stimulation research. *The Journal of ECT*, 22(3), 176–178. <https://doi.org/10.1097/01.yct.0000235924.60364.27>
- Siebner, H., & Rothwell, J. (2003). Transcranial magnetic stimulation: New insights into representational cortical plasticity. *Experimental Brain Research*, 148, 1–16.
- Skipper, J. I., Devlin, J. T., & Lametti, D. R. (2017). The hearing ear is always found close to the speaking tongue: Review of the role of the motor system in speech perception. *Brain and Language*, 164, 77–105.
- Tang, Y., Ying, C., Wang, J., Jiao, X., Qian, Z., Zhang, T., ... Wang, J. (2018). Precise theta burst transcranial magnetic stimulation selectively reduced duration-related mismatch negativity. *Biological Psychology*, 137, 125–132.

- Thielscher, A., Antunes, A., & Saturnino, G. B. (2015). Field modeling for transcranial magnetic stimulation: A useful tool to understand the physiological effects of TMS? 37th Annual International Conference of the IEEE Engineering in Medicine and Biology Society, 222–225. <https://doi.org/10.1109/EMBC.2015.7318340>
- Turkeltaub, P. E., Branch Coslett, H., Thomas, A. L., Faseyitan, O., Benson, J., Norise, C., & Hamilton, R. H. (2012). The right hemisphere is not unitary in its role in aphasia recovery. *Cortex*, 48, 1179–1186.
- Turken, A. U., & Dronkers, N. F. (2011). The neural architecture of the language comprehension network: Converging evidence from lesion and connectivity analyses. *Frontiers in Systems Neuroscience*, 5, 1.
- Tzourio-Mazoyer, N., Perrone-Bertolotti, M., Jobard, G., Mazoyer, B., & Baciau, M. (2017). Multi-factorial modulation of hemispheric specialization and plasticity for language in healthy and pathological conditions: A review. *Cortex*, 86, 314–339.
- Vaden, K. I., Kuchinsky, S. E., Cute, S. L., Ahlstrom, J. B., Dubno, J. R., & Eckert, M. A. (2013). The cingulo-opercular network provides word-recognition benefit. *The Journal of Neuroscience*, 33, 18979–18986.
- Vaidya, A. R., Pujara, M. S., Petrides, M., Murray, E. A., & Fellows, L. K. (2019). Lesion studies in contemporary neuroscience. *Trends in Cognitive Sciences*, 23, 653–671.
- Winhuisen, L., Thiel, A., Schumacher, B., Kessler, J., Rudolf, J., Haupt, W. F., & Heiss, W. D. (2005). Role of the contralateral inferior frontal gyrus in recovery of language function in poststroke aphasia: A combined repetitive transcranial magnetic stimulation and positron emission tomography study. *Stroke*, 36, 1759–1763.
- Wischnewski, M., & Schutter, D. J. L. G. (2015). Efficacy and time course of theta burst stimulation in healthy humans. *Brain Stimulation*, 8, 685–692.
- Woźniak-Kwaśniewska, A., Szekely, D., Aussedat, P., Bougerol, T., & David, O. (2014). Changes of oscillatory brain activity induced by repetitive transcranial magnetic stimulation of the left dorsolateral prefrontal cortex in healthy subjects. *NeuroImage*, 88, 91–99.

How to cite this article: Klaus J, Schutter DJLG, Piai V. Transient perturbation of the left temporal cortex evokes plasticity-related reconfiguration of the lexical network. *Hum Brain Mapp*. 2020;41:1061–1071. <https://doi.org/10.1002/hbm.24860>